

Analysis and Evaluation the Effect of Electrode Films on the SAW Torque Sensitivity

Yanping Fan^{a,*}, Yajun Liu^a, Qiang Xiao^b, Xiaoxin Ma^b, Pengfei Sun^c, and Xiaojun Ji^b

^a*School of Optical-Electrical and Computer Engineering, University of Shanghai for Science and Technology, Shanghai, 200093 China*

^b*School of Electronic Information and Electrical Engineering, Shanghai Jiao Tong University, Shanghai, 200240 China*

^c*Institute of Machinery Manufacturing Technology, China Academy of Engineering Physics, Mianyang, 621900 China*

**e-mail: fypofcas@163.com*

Received April 5, 2019; revised September 4, 2019; accepted September 5, 2019

Abstract—The surface acoustic wave (SAW) sensor has been widely used to measure torque, and the temperature effect on torque sensitivity has been taken into account. However, few studies have been devoted to the influence of electrode on the torque sensitivity. In order to design a SAW torque sensor with high performance, it is necessary to analyze the effect of electrode. We adopt the Mindlin's thin plate equations as a boundary condition due to the electrode, propose a method to evaluate the effect of electrode and make a comparison between our calculation and experimental results. Then, we obtain the frequency shifts with different electrode materials when the applied torque is zero. Finally, we evaluate the torque sensitivity with the effect of electrode and obtain the result with the errors about 1.7 and 7.6% compared with experimental data. The errors have been improved greatly with respect to the calculation ignoring electrode effect, about 30%. However, the analysis is valid only under the condition that the thickness of electrode is relatively small, which is satisfied in the general conditions.

Keywords: SAW, electrode, perturbation theory, torque sensor

DOI: 10.1134/S1063771020010042

1. INTRODUCTION

It's important to measure the torque accurately in many cases such as designing automotive gearwheels [1], examining axial multipiston pumps [2]. Piezoelectric crystal resonators are now widely used as frequency generators, duplexers and sensors [3]. Surface acoustic wave (SAW) devices have a large readout distance and an energy supply of the devices only by an external radio frequency (RF) module [4] and have been used to measure torque successfully [5, 6]. The theoretical model describing temperature characteristics of the SAW torque sensor had been built and a configuration of the sensor that had reduced temperature variation of the sensitivity to torque was suggested [7]. The common structure of a SAW torque sensor is a certain thickness piezoelectric crystal substrate covered by a thin film of metal electrode. However, few studies have investigated the effect of electrode films on SAW torque sensitivity. We should take the influence of electrodes into account to design a high quality of SAW torque sensor.

Stresses in thin films are a common occurrence for all metalization processes. The most obvious source of such stress is the difference in thermal expansion between the film and the substrate. This source of

stress is well-defined and predictable [8]. Unfortunately, the source of the largest component of thin-film stress is less well-defined [9]. It is called intrinsic stress and is related to nucleation and grain boundary effects during growth of the film and during subsequent thermal cycling [9]. These intrinsic stresses, which result from the deposition of the film, in turn, cause a residual stress state to exist in the substrate in order to the entire system (film plus substrate) remains in equilibrium [10]. The combined intrinsic plus residual stress state has an influence on the velocity [11] and resonant frequency. Some researchers adopted Equivalent-Circuit Model and FEM methods to analysis the electrode effect [12, 13]. These methods are complicate and time consuming. Thus, we adopted the Mindlin's thin plate theory to analysis the electrode effect. The main work of our paper is to analyze the influence of intrinsic stresses, due to the thin film electrodes, on the SAW torque sensitivity.

2. THE ELECTRODE INFLUENCE ON THE TORQUE SENSITIVITY

The structure of crystal resonator is that the thin periodic electrode films or interdigital covered on a semi-infinite crystal substrate with the width and

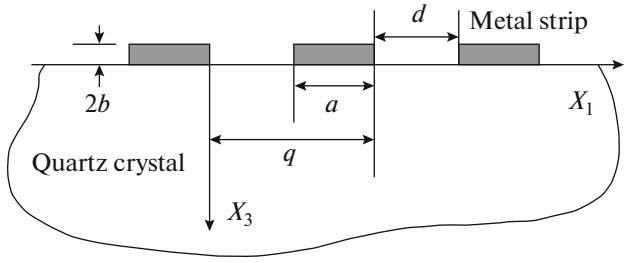


Fig. 1. The structure of crystal resonator.

height of the electrode films are a and $2b$, as Fig. 1 shows. The period of the electrode films is q and the interval between each electrode is d . In order to simplify the analysis process, we take the interval of metal strips equal to the width of metal strip, and the periodicity of electrode coincides with the wavelength of surface acoustic wave.

The covered electrode films will induce intrinsic stresses and residual stresses at the interface between crystal and metal strip. Moreover, if the metal strip is very thin compared with the SAW wavelength, just as $\pi/\xi \gg b$, the mechanical metal strip effect can be described by a certain thin-plate equations. The approximate plate equation for a thin isotropic film plated on a substrate may be written in the form [14]:

$$T_{3j}^e = -\delta_{jM} 2b\mu \left[\frac{3\lambda + 2\mu}{\lambda + 2\mu} U_{N,NM}^e + U_{M,NN}^e \right] + 2b\rho^e \ddot{U}_j^e, \quad (1)$$

where the Cartesian tensor notion is used. The superscript e denotes the elastic stress and displacement in the metal strip and in the above equation. U_N^e , $2b$, ρ^e , λ , μ are the mechanical displacement, height of metal film, metal mass density, the Lamé constants, respectively. δ_{jM} is the Kronecker delta. The subscripts M and N take the values 1 and 2 but not 3, and T_{3j}^e denotes the components of the traction vector at the surface of the substrate. At the interface of the crystal substrate and metal strip, we can get the boundary conditions as:

$$\begin{aligned} \bar{U}_m &= U_m^e, \quad \bar{T}_3 = T_3^e, \quad \bar{T}_4 = T_4^e, \quad \bar{T}_5 = T_5^e \\ &\text{at } X_3 = 0, \quad d \leq X_1 \leq q, \\ T_3 &= 0, \quad T_4 = 0, \quad T_5 = 0 \quad \text{at } X_3 = 0, \quad 0 \leq X_1 \leq d, \end{aligned} \quad (2)$$

where the ‘‘barred’’ quantities denote the variable under metal strip. Finally, we can obtain the mechanical displacement and electric potential as:

$$\begin{cases} U_m = \left[\sum_{t=1}^4 C^t B_m^t e^{i\beta_t \xi X_3} \right] e^{i(\xi X_1 - \omega t)}, \\ \varphi = \left[\sum_{t=1}^4 C^t e^{i\beta_t \xi X_3} \right] e^{i(\xi X_1 - \omega t)} \end{cases} \quad \text{at } X_3 = 0, 0 \leq X_1 \leq d, \quad (3)$$

$$\begin{cases} \bar{U}_m = \left[\sum_{t=1}^4 \bar{C}^t \bar{B}_m^t e^{i\bar{\beta}_t \xi X_3} \right] e^{i(\xi X_1 - \omega t)}, \\ \bar{\varphi} = \left[\sum_{t=1}^4 \bar{C}^t e^{i\bar{\beta}_t \xi X_3} \right] e^{i(\xi X_1 - \omega t)} \end{cases} \quad \text{at } X_3 = 0, d \leq X_1 \leq q,$$

where C^t , B_m^t , φ , β , ξ , ω , t are linear combination coefficients, amplitude ratios, electric potential, mechanical displacement amplitude, decaying index, propagation constant, resonance frequency, time, respectively. Since static mechanical stress bias in a quartz resonator changes the resonant frequency through finite strain effects [9], the electrode intrinsic stresses will cause resonant frequency shifts and it will be included in the total frequency change to a SAW torque sensor. Hence, we utilize the perturbation theory to analyze the influence of electrode on torque sensitivity. According to the perturbation theory, the applied torque changes the elastic constants. The effective elastic constants are [15]:

$$G_{klmn} = c_{klmn} + \hat{c}_{klmn}, \quad (4)$$

where G_{klmn} is the effective elastic constants, \hat{c}_{klmn} is the perturbation bias, which has to do with the applied torque:

$$\hat{c}_{klmn} = \delta_{ln}^1 T_{km}^1 + c_{klmns} S_{sw}^1 + c_{klmns} w_{l,t} + c_{kltn} w_{m,t}, \quad (5)$$

where T_{km}^1 , S_{sw}^1 , $w_{l,t}$ are the biasing stress, strain, and displacement gradients in the biasing state of the SAW torque sensor substrate; c_{klmns} is the third-order elastic constants. The surface acoustic wave, propagating along the direction X_1 , varies periodic and the metal strips are arrayed with the same periodicity. For simplicity, we just consider the integral range within a wavelength. For the mechanical displacement is different in the area with and without metal electrode covered, there are two different calculations in an electrode period. The area without electrode satisfies the boundary condition that the surface of piezoelectric plate is traction free, and hence the divergence theorem can be applied in the area. After using Green’s identity in the perturbation analysis for frequency shifts in resonators [15], we have:

$$\begin{aligned} &\rho(\omega^2 - \omega_0^2) \left(\int_{V_1} U_j U_j^* dV + \int_{V_2} \bar{U}_j \bar{U}_j^* dV \right) \\ &= \int_S \int_{X_1=0}^{X_1=\pi/2\xi} \hat{c}_{ijkl} U_{l,k} U_{j,i}^* dX_1 ds - \int_S \int_{X_1=\pi/2\xi} \hat{c}_{ijkl} \bar{U}_{l,ki} \bar{U}_j^* dX_1 ds, \end{aligned} \quad (6)$$

in which ω and ω_0 are resonant frequency under conditions that with and without torque applied. Let the applied torque generating unit strain at $\pm 45^\circ$ along the shaft axis. Then by substituting the coefficients obtained in Eq. (3) into Eq. (6), we can get both sides of the integral respectively as:

$$\begin{aligned} \int_{V_1} U_j U_j^* dV &= \int_{V_1} \left[\sum_{m=1}^4 C^m B_j^m e^{i\beta_m \xi X_3} \right] e^{i(\xi X_1 - \omega t)} \\ &\times \left[\sum_{n=1}^4 C^{n*} B_j^{n*} e^{-i\beta_n^* \xi X_3} \right] e^{i(-\xi X_1 + \omega t)} dV \\ &= \frac{i\pi}{2\xi^2} \sum_{m=1}^4 \sum_{n=1}^4 \frac{C^m B_j^m C^{n*} B_j^{n*}}{\beta_n^* - \beta_m} = KM, \end{aligned} \quad (7)$$

$$\begin{aligned} \int_{V_2} U_j U_j^* dV &= \int_{V_2} \left[\sum_{m=1}^4 \bar{C}^m \bar{B}_j^m e^{i\bar{\beta}_m \xi X_3} \right] e^{i(\xi X_1 - \omega t)} \\ &\times \left[\sum_{n=1}^4 \bar{C}^{n*} \bar{B}_j^{n*} e^{-i\bar{\beta}_n^* \xi X_3} \right] e^{i(-\xi X_1 + \omega t)} dV \\ &= \frac{i\pi}{2\xi^2} \sum_{m=1}^4 \sum_{n=1}^4 \frac{\bar{C}^m \bar{B}_j^m \bar{C}^{n*} \bar{B}_j^{n*}}{\bar{\beta}_n^* - \bar{\beta}_m} = KN, \end{aligned} \quad (8)$$

$$\begin{aligned} &\int_S \int_{X_1=0}^{X_1=\pi/2\xi} \hat{c}_{ijkl} U_{l,k} U_{j,i}^* dX_1 ds \\ &= \int_0^{\pi/2\xi} dX_1 \int_{-\infty}^{\infty} \hat{c}_{ijkl} \left[\sum_{m=1}^4 \xi^2 p_k^m C^m B_l^m e^{i\beta_m \xi X_3} \right] e^{i(\xi X_1 - \omega t)} \\ &\times \left[\sum_{n=1}^4 p_i^{n*} C^{n*} B_j^{n*} e^{-i\beta_n^* \xi X_3} \right] e^{i(-\xi X_1 + \omega t)} dX_3 \\ &= -\frac{i\pi}{2} \hat{c}_{ijkl} \sum_{m=1}^4 \sum_{n=1}^4 \frac{p_k^m C^m B_l^m p_i^{n*} C^{n*} B_j^{n*}}{\beta_m - \beta_n^*} = KU, \end{aligned} \quad (9)$$

$$\begin{aligned} &\int_S \int_{X_1=\pi/2\xi}^{X_1=\pi/\xi} \hat{c}_{ijkl} \bar{U}_{l,ki} \bar{U}_j^* dX_1 ds \\ &= \int_{\pi/2\xi}^{\pi/\xi} dX_1 \int_{-\infty}^{\infty} \hat{c}_{ijkl} \left[\sum_{m=1}^4 -\xi^2 \bar{p}_k^m \bar{p}_i^m \bar{C}^m \bar{B}_l^m e^{i\bar{\beta}_m \xi X_3} \right] \\ &\times e^{i(\xi X_1 - \omega t)} \left[\sum_{n=1}^4 \bar{C}^{n*} \bar{B}_j^{n*} e^{-i\bar{\beta}_n^* \xi X_3} \right] e^{i(-\xi X_1 + \omega t)} dX_3 \\ &= \frac{i\pi}{2} \hat{c}_{ijkl} \sum_{m=1}^4 \sum_{n=1}^4 \frac{\bar{p}_k^m \bar{p}_i^m \bar{C}^m \bar{B}_l^m \bar{C}^{n*} \bar{B}_j^{n*}}{\bar{\beta}_m - \bar{\beta}_n^*} = KV, \end{aligned} \quad (10)$$

where KM , KN , KU and KV are four values, and $p_1^m = 1, p_2^m = 0, p_3^m = \beta_m$. Consequently, after considering the electrode, the first-order description of frequency shifts due to applied torque including the influence of electrode can be expressed as:

Table 1. The strain sensitivity of the different orientations

Orientation	Shvetsov's calculation	Our calculation
(0°, 55°, 90°)	-2.4 kHz/ $\mu\epsilon$	-2.6 kHz/ $\mu\epsilon$
(0°, 110°, 55°)	-2 kHz/ $\mu\epsilon$	-2.05 kHz/ $\mu\epsilon$
(0°, 40°, 0°)	1.3 kHz/ $\mu\epsilon$	1.08 kHz/ $\mu\epsilon$
(30°, 60°, 70°)	-2.3 kHz/ $\mu\epsilon$	-2.4 kHz/ $\mu\epsilon$
(30°, 90°, 125°)	-1.7 kHz/ $\mu\epsilon$	-1.74 kHz/ $\mu\epsilon$

$$\Delta f = \frac{1}{4\pi\omega_0\rho} \frac{KU - KV}{KM + KN}. \quad (11)$$

Before verifying the effectiveness of our proposed method to predict the torque sensitivity with the influence of electrode, we first calculate the torque sensitivity ignoring the effect of electrode just let $b = 0$ and make a comparison with [16]. The sensitivity is given in kHz per micro strain value (kHz/"microstrain" = kHz/ $\mu\epsilon$) for a pair of resonator working in a differential mode with initial resonance frequencies 200 and 201 MHz, respectively. The results are listed in Table 1.

From Table 1 we can find that the designed method to predict the torque sensitivity is effective when ignoring the influence of electrode. As we know that $\Delta f/f = \Delta v/v$. In order to verify our method, we take a ST cut of quartz for example, on which aluminum electrodes are plated and the applied torque is zero. The quartz material constants and the aluminum constants are taken as [17] used. The electrode thickness is 50 nm and the operating frequency is $f = 153$ MHz. The calculated results are shown in Fig. 2 with the propagation direction varies from 0 to 7 degree. Line *a* stands for theoretical predictions of SAW velocity considering the influence of the aluminum electrode; line *b* stands for theoretical predictions of SAW velocity eliminating the influence of electrode; line *c* and *d* are Minowa's theoretical predictions and experimental results, respectively [17]. It's clearly shown in Fig. 2 that there is a large discrepancy between theoretical calculation without considering the effect of electrode influence and Minowa's experimental data. The electrode films caused a velocity error about 5 m/s. Considering the electrode influence, the calculated SAW velocity values show a good consistence with the Minowa's experimental data [17]. The reason why line *a* has a relatively larger error than the Minowa's theoretical predictions to the experimental results is that the influence of thermal expansion between the film and the substrate is ignored. At the same time, we calculate the relative frequency shifts $\Delta f/f$ with different electrode materials along different propagation direc-

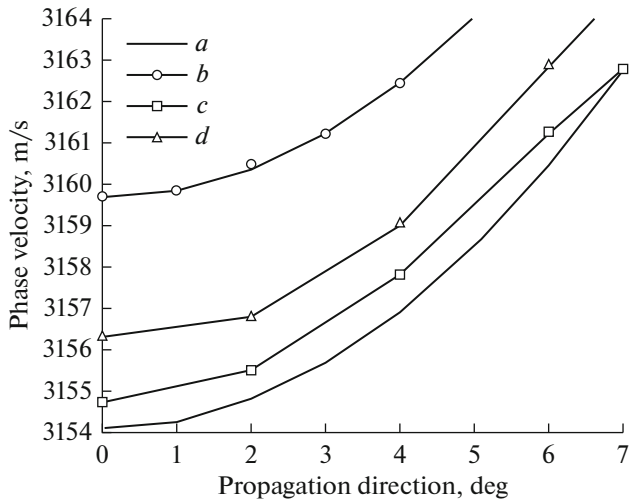


Fig. 2. The SAW velocity propagation along different direction. The line *a* stands for our theoretical predictions of SAW velocity considering the influence of the aluminum electrode; line *b* stands for our theoretical predictions of SAW velocity eliminating the influence of electrode; line *c* and line *d* are Minowa’s theoretical predictions and experimental results, respectively.

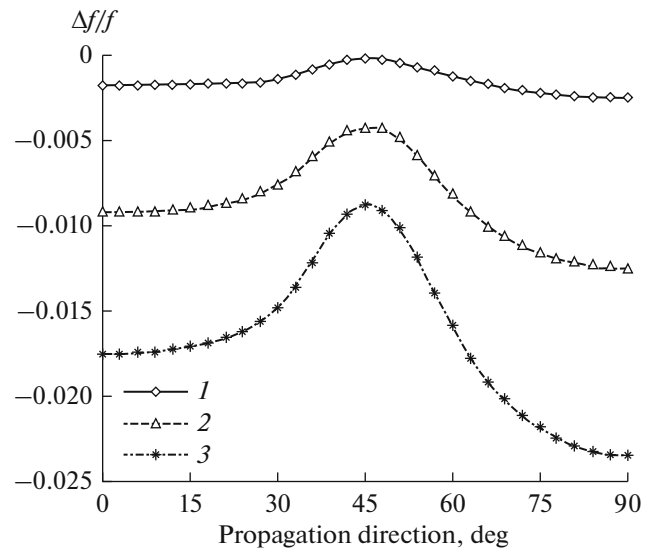


Fig. 3. The relative frequency shifts with different electrode materials along different propagation direction. The line *1* stands for aluminum electrode; line *2* stands for silver electrode; line *3* stands for gold electrode.

tion. Line *1* stands for aluminum electrode; line *2* stands for silver electrode; line *3* stands for gold electrode, as Fig. 3 shows. It can be found that both cut angle and the electrode materials have an influence on the SAW resonant frequency shift. Different electrode materials cause different frequency shifts. The influence of gold electrode is greater than aluminum and silver. The reason is that gold has a larger density than the other two materials and has a larger press applied on the quartz. Thus, the material and the thickness of metal strip have an influence on the performance of manufactured SAW devices.

Finally, we predict the effect of electrodes on the torque sensitivity by taking the same conditions as [16] process in calculation. We obtain the relative torque sensitivity, which is related to sensitivity of same sensor based on ST-X-cut, listed in Table 2.

It can be found that our calculation is more close to the Shvetsov’s experimental results when the thickness of electrode is relatively small. The error has been improved greatly with respect to the Shvetsov’s calculation, about 18%. Therefore, it is safe to predict the torque sensitivity when covered with electrode if the thickness of electrode is very thin compared with the SAW wavelength. When the thickness is large, our method will not be applicable. For example, when the ratio of thickness to SAW wavelength is 4% for the $yx1/20^\circ/50^\circ$ cut, the relative torque sensitivity of our calculation is 6.29, but the experimental result is 3.1. The reason of the result is that the boundary condition of equation (1) is not suitable anymore for the large thickness of metal strips and needs same variation. So, in the design SAW torque sensor process with relatively thin electrode thickness to SAW wavelength, we pro-

Table 2. The relative torque sensitivity

Cuts and electrodes thickness to wavelength	Our calculation				Shvetsov’s result		
	ignoring electrode		with electrode		calculation		experimental
	value	error	value	error	value	error	
$yx1/-40^\circ$ 1.4%	1.69	29.6%	2.36	1.7%	1.9	20%	2.4
$yx1/-30^\circ$ 2.2%	1.57	37.2%	2.69	7.6%	1.7	32%	2.5

vide a more accurate prediction of SAW torque sensitivity, which makes our design more acceptable.

3. CONCLUSION

We derive the SAW velocity affected by the covering metal electrode strips by taking the metal's strain as a boundary condition, obtain the frequency shifts due to the effect of electrode, and utilize the Sinha-Tiersten's perturbation to analyze influence of electrode on the SAW torque sensitivity. By comparing the calculated result of our method with experimental data, it verifies that we can get a more accurate result when the thickness to SAW wavelength is relatively small. However, when the electrode thickness is relatively large, the error of our result is unacceptable. The proposed method can only be applied to the condition that the thickness to wavelength ratio is small. Our next work will focus on the large thickness electrode influence on the SAW property.

FUNDING

This work was supported by the Natural Science Foundation of China, under Grant nos. 51705326 and 51475306.

REFERENCES

1. A. Dočekal, V. Dynybyl, M. Kreidl, R. Šmíd, and P. Šmíd, *Meas. Sci. Rev.* **8**, 42 (2008).
2. T. Zloto, *Meas. Sci. Rev.* **1**, 123 (2001).
3. X. Ji, Y. Fan, T. Han, and P. Cai, *Acoust. Phys.* **62**, 160 (2016)
4. Y. Fan, X. Ji, P. Cai, and Q. Lu, *Meas. Sci. Rev.* **13**, 25 (2013).
5. V. Kalinin, R. Lohr, A. Leigh, and G. Bown, in *Proc. 2007 IEEE Int. Frequency Control Symposium* (Geneva, 2007), p. 499.
6. Y. Fan and X. Ji, *Acoust. Phys.* **64**, 122 (2018).
7. J. Beckley, V. Kalinin, M. Lee, and K. Voliansky, in *Proc. IEEE Int. Frequency Control Symposium and PDA Exhibition* (New Orleans, LA, 2002), p. 202.
8. S. G. Suchkov and D. A. Barinov, *J. Commun. Technol. Electron.* **47**, 458 (2002).
9. E. EerNisse, in *Proc. IEEE 29th Int. Frequency Control Symposium* (Atlantic City, NJ, 1975), p. 1.
10. H. Tiersten, B. Sinha, and T. Meeker, *J. Appl. Phys.* **52**, 5614 (1981).
11. P. Singh and R. Yadava, *Meas. Sci. Technol.* **22** (2), 1 (2011).
12. R. Meftah and Y. Meyer, *Mech. Adv. Mater. Struct.* **9**, 774 (2013).
13. C. Sun, Z. Chen, R. Tong, H. Xu, and C. Han, in *Proc. 2015 Symposium on Piezoelectricity, Acoustic Waves, and Device Applications* (Jinan, 2015), p. 120.
14. H. Tiersten and B. Sinha, *J. Appl. Phys.* **49**, 87 (1978)
15. H. Tiersten, *J. Acoust. Soc. Am.* **64**, 832 (1978).
16. A. Shvetsov, S. Zhgoon, A. Lonsdale, and S. Sandacci, in *Proc. IEEE Int. Ultrasonics Symposium* (San Diego, CA, 2010), p. 1250.
17. J. Minowa, *Electr. Commun. Lab. Rev.* **26**, 797 (1978).